Phenomenological technique for prediction of cavitation erosion performance

B.G. Gireń *, A. Welzant, P. Baran

Institute of Mechatronics and Informatics, University of Economics,
ul. Garbary 2, 85-229 Bydgoszcz, Poland
* Corresponding e-mail address: boleslaw.giren@byd.pl
ORCID identifier: https://orcid.org/0000-0002-9315-0109 (B.G.G.)

ABSTRACT

Purpose: Major aim of the work was to formulate 2-parameters models of the cavitation erosion process and to bring about the particular methods for prediction of its performance with due calculation formulas.

Design/methodology/approach: Phenomenological model of the erosion supplemented with functional relationships between calculation parameters and the strength parameters stand for the foundations of the method. Having assumed the probabilistic nature of the process and fatigue regime of the material destruction, the volume loss in time has been determined as proportional to the integral of the appropriate probability function. Correlations between parameters have been derived by adjusting the computed erosion curves to the experimental ones for the vast diversity of the cases.

Findings: Two different formulas for the volume loss of the material in time under cavitation loading have been derived.

Research limitations/implications: Results obtained from both the International Cavitation Erosion Test program as well as the own experiments carried out at the rotating disk set-up supplied necessary experimental data. Preliminary verification of the method soundness was completed. Assumption on the independence of the calculation parameters on the loading conditions have been taken. The approach is valid provided the defined relationships are also independent on the type and amplitude of the loading.

Practical implications: Achieving the objectives is expected to result in developing a technique for assessment of the material damage under cavitation loadings. Numerical implementation of the model completed with the derived functional relationships stand for a tool, enabling a prospective user to predict the material performance under defined cavitation loading.

Originality/value: New formulas for calculating the efficiency of cavitation erosion, inferred from the models of high physical clarity are the original contribution to the methodology and techniques concerned.

Keywords: Cavitation erosion, Material performance, Performance evaluation, Wear, Erosion process modelling, International Cavitation Erosion Test

Reference to this paper should be given in the following way:

B.G. Gireń, A. Welzant, P. Baran, Phenomenological technique for prediction of cavitation erosion performance, Archives of Materials Science and Engineering 104/2 (2020) 69-85. DOI: https://doi.org/10.5604/01.3001.0014.4896

METHODOLOGY OF RESEARCH, ANALYSIS AND MODELLING

RESEARCH PAPER

1. Introduction

1.1. Domain of the issues

Cavitation erosion in the initial stage is featured by substantial variety of the volume loss due to the random nature of the process. Poor repeatability of the effects of the loading impulses lead to major diversity in the sets of the results obtained in the same conditions, the feature causing the prediction of the process difficult [1]. Cavitation erosion may be a vital problem in liquid-flow systems, such as ship propellers, hydraulic turbines or valves, being a reason of major concern for equipment designers and users (e.g. [2,3]). Defects occurring due to cavitation action result in decreasing the efficiency of operating machines and cause the frequent maintenance and repairs are necessary. Search for the valid tool for prediction of the erosion performance in defined conditions is thus accounted for reduction of the exploitation risk as well as decrease in costs of designing, maintenance and repair of the hydro-turbines and other devices. Getting knowledge on the dependence of the cavitation erosion of the materials on mechanical properties and the structure and intensity of the loadings would allow to predict the performance of the process, which is essential issue from engineering point of view.

To cope with the problem the huge conceptual and numerical efforts are required. Herein, an implementation of the simple mathematical approach for approximate quantification of the cavitation erosion supplemented with functional relationships between computational parameters and the strength parameters of the material at chosen loading conditions is proposed as a tool for assessment the process performance in the initial stage.

Core issue of the present work is to formulate and develop a method for quantification of the cavitation erosion in the initial stages of the process – extended up to the middle of accelerated erosion stage as well as to assess the possible uncertainty and validity of both experimental data and the results of erosion prediction. The considerations performed refer to metallic alloys. Foundations of the method comprise the simple two-parameter formula for evaluation of a random damage of the material and the phenomenological procedure to disclose the formulas for determining the parameters values. The basis of the analysis carried out were experimental results obtained at 9 laboratories during the International Cavitation Erosion Test [1,4,5] realisation as well as the results of the own experiments carried out at the rotating disk set-up in the Szewalski Institute of Fluid-Flow Machinery Polish Academy of Sciences.

1.2. Quantification aspects of the process and the resulting problems

Cavitation erosion is defined as damage of material surface layers in liquid environment, caused by local impingements of microjets or shock waves. The latter are the result of implosions of gas-vapor bubbles, which arise when pressure of the surrounding medium is low. Followingly the bubbles shrink under the increased pressure. Variation of liquid pressure value may be a function of time or position – thus the bubble can bear the loadings in situ or being transported along the stream of varying pressure and under the forces arising from bubble implosions, especially as microjets or shock waves are generated [6,7]. The process depends on the type and amplitude of the loadings, their dynamics and spatial distribution of acting forces, surface morphology of the material, its microstructure, phase and chemical composition, residual stresses in the body and the resulting strength parameters. The influence of various determinants on the process performance was investigated, e.g. in [7-12]. During material disintegration specific stages may be distinguished: energy accumulation period followed by the volume loss acceleration and quasi-stabilisation stages [13,14]. At the beginning of the erosion the internal stresses and deformations are accumulated without substantial mass loss. Discernible indentations are formed in the surface layer due to plastic deformations. Their compaction is used as a measure of material damage in this period. That process is prior to cracking and extracting the solid pieces. Randomness of the loadings [15], microstructure and initial conditions stand for the random nature of the process in time and space domains.

Numerous attempts to develop efficient method for prediction of cavitation erosion have been reported, e.g. in [16-25]. However, in most cases the results achieved did not account for incubation, acceleration and long-term exposure periods with equal precision and were not applicable due to hardly achievable physical data on process conditions. The latter forced the considerations to be confined to the incubation period of the erosion, e.g. by modelling cavitation impingements on the solid surface [26-28], or by finding scaling or similarity laws, e.g. in [29-34]. An issue, important from the practical point of view is that precise prediction of cavitation erosion is difficult due to high sensitivity of the process. Substantial scatter in material volume being extracted in conditions differing only by quality of the loadings was observed [1]. According to considerations carried out in [35] the relationship between characteristics of the loading, i.e. its structure and intensity and cavitation damage seems to be crucial. However, not negligible ambiguities arise from various regimes of the

damage process: fatigue or hardening regime [36] or due to the other factors possibly driving the process, e.g. the deteriorative role of hydrogen [37]; forced diffusion of hydrogen from environmental medium under cavitation conditions contributes to acceleration of damage process.

1.3. Aims and scope

Major aim of the present work was to formulate a particular method for prediction of the cavitation erosion performance in the initial stages of the process and to develop the corresponding calculation tool. Phenomenological model of the erosion and the resulting two-parameters formula, supplemented with functional relationships between calculation and the strength parameters of the materials, derived for chosen loading conditions stand for the foundations of the method. Two different formulas for the material volume loss as a function of time, obtained from two simple phenomenological models with due relationships between calculation and the strength parameters have been derived. The latter dependencies have been achieved by completing procedure of adjusting the computed erosion curves to the experimental data points for the vast diversity of the cases and subsequently revealing the existing correlations. Results obtained from both the International Cavitation Erosion Test program as well as the own experiments carried out at the rotating disk set-up supplied necessary experimental data. Preliminary verifications of each implementation of the method soundness were also completed. Achieving the objectives would contribute to develop a technique for assessment of the material damage under optional cavitation loadings.

2. Outline of the phenomenological technique for prediction of cavitation erosion performance

If the erosion is related to energy consumption in constituent processes of stochastic nature, such as plastic deformations under loading impacts prior to microcracks inception, microcrack generation and retarding processes, e.g. generation of plastic zones at the microcrack tips and energy dissipation during interaction of the surface layer with the environment, the following assumption on the damage rate can be accepted: the higher difference between the sum of the rates of energy absorption at plastic deformations and microcrack generation and the rate of energy consumption in retarding processes, the higher the

sum of the rates of energy expenditure at the critical cracks development and loss of the energy accumulated in extracted debris. The latter sum is postulated to be proportional to the yield of the process [23]. Generation of plastic zones at the microcrack tips and energy dissipation during interaction of the surface layer with the environment are considered as retarding processes. Under additional assumptions: (1) the retarding processes are not effective and may be omitted, (2) the constituent subprocesses of the erosion are not distinguished, (3) parameters of the probability functions for the processes are assumed constant, related to given material properties and not related to the loading, (4) the efficiency of the process is proportional to the loading intensity, one may submit the concept the erosion can be simply proportional to the integral of the probability function. Due to its formulation, the model disregards the space resolution of the damage topography. Parameters of the probability functions for the constituent processes and proportional coefficient may be only derived by comparisons to the experimental data, thus, from that point of view the model is of phenomenological nature.

Prognostic system developed on the basis of the presented model requires the functional dependencies between parameters of the probability distribution functions and material strength parameters inferred in phenomenological way. Methodological concept consists in adjusting the theoretical erosion curves to experimental results for each individual case by variation and appropriate selection of the calculation parameters values. Matching the calculation and strength parameters was expected to reveal the functional relationships between them. Having the relationships found, the erosion process of any known material in any known loading conditions could be determined. Numerical implementation of the model completed with the derived functional relationships stand for a tool, enabling a prospective user to predict the material performance under defined cavitation loading. The approach is valid provided the defined relationships are independent on the type and amplitude of the loading.

3. Theoretical and experimental foundations of the method

Randomness of impulses with respect to time, place and height, impact angles and local properties of material microstructure makes the cavitation erosion a stochastic process. Its effectiveness depends both on the loading characteristics and characteristics of the eroded body, defined by its chemical composition, microstructure and

physical state. Resulted initial properties of the target may be of paramount importance in the incubation period of the erosion. Therefore, it seems to be justified to relate the erosion process to the probability of the material disintegration under external forces. In probabilistic view, the temporary rate of the erosion should be proportional to the variation of the probability $p(t)$ of the extraction of elementary material volume over unit area in unit time under unit loading $\frac{dv}{dt} = Ip(t)$, where v is a volume loss and I means the average loading measure. Then, the average value of the erosion may be attained from multiplying it by the loading and subsequent integrating the expression over the time:

$$v = I \int_0^t p(\tau)d\tau \qquad (1)$$

Another model reasoning may launch from the assumption that material volume loss u_i under single loading impulse $f(t)$ during its lasting results from the convolution: $u_i \sim \int_{t_{i-1}}^{t_i} f(\tau)\varphi(t_i - \tau)d\tau$, where t, τ means time, $(t_{i-1}; t_i)$ is the duration of the impulse, $f(t)$ is the characteristics of the loading impulse and $\varphi(t)$ means the probability density function of the extraction of elementary material volume over unit area in unit time under unit loading. The overall volume loss is the sum of the losses caused by subsequent impulses: $u = \sum_i u_i$. Performing the Laplace transformation and applying the Borel statement one obtains within the summation limit the final result: $u = \bar{f} \int_0^t p(\tau)d\tau$, the same as in (1).

The similar formula may also be found if considerations refer to very thin surface layer, i.e. the surface layer of the thickness so low that effective impact loading results in detaching the excerpt of the whole cross section of the layer. This time, a relation for decrease of the partition of the layer removed: $x(t) \sim \int_0^t x(\tau)\varphi(t - \tau)d\tau$ may be simplified to the form:

$$x(t) = \varepsilon \int_0^t H(t - \tau)\varphi(\tau)d\tau \qquad (2)$$

where H is a Heaviside function and ε is a coefficient dependent on the loading conditions.

Parameters of the distribution function are not known a priori, than necessary supplemental tasks involve determining the functional relationships between the probability function parameters and measurable strength parameters of the materials for chosen cavitation loading conditions.

3.1. Simple two-parameters models of the process

The process may perform along one of the damage regimes: fatigue or hardening regime [36], however, opinion on predominant meaning of the fatigue regime was inferred, i.e. from strong correlation between cavitation damage and fatigue strength of the material [8,38]. Fatigue-like damage within incubation period of the erosion follows the Miner's law of impact loads, irrespective on cavitation conditions and type of material [39].

Keeping in mind the stochastic nature of the process, it seems admissible to regard the probability of the material disintegration under external forces as a function of the temporal density of the hypothetical energy trapping points within the surface layer of the solid body. Integral of that probability over the time may be assumed to be proportional to the volume loss. The formula for probability function depends on the model assumptions. Hence, it can be adopted from excitation energy migration theory, developed, i.e. in [40]. Alternatively, taking into account the fatigue strength is of paramount meaning for cavitation erosion resistance of the material and the adequacy of the Weibull distribution to describe the random fatigue phenomena [41] it could be implied the assumption that volume loss of the material under the unit area of the sample at the initial stage of the erosion is proportional to the integral of the Weibull cumulative distribution function over the time, multiplied by the coefficient dependent on the loading intensity value. There was reported that statistics of some variables referring to the cavitation erosion process or to the random processes of cavitation loading might follow the Weibull distribution function [42-45].

Model inspired by Forster energy migration theory

The following assumptions have been taken and included implicitly in the model formulation:

- mass loss rate during the process is driven by: – the value of the impulses energy absorbed and accumulated, which is related to the temporal density of the energy trapping points and the hysteresis loop, and – the value of the threshold energy for crack inception, thus resulting in material disintegration. In mathematical formulation, the specified values are represented by two independent parameters, which are assumed constant for given material;

- mass loss rate during the process is proportional to average intensity of cavitation loading, which appear in the mathematical formulation as coefficient of proportionality;

- in time up to the maximum rate of the erosion is achieved both the density of the energy trapping points and the energy accumulation rate achieve the values to provide the remove probability of all elementary pieces from the surface layer of the material;
- target material and space distribution of the impulses are considered statistically homogenous;
- decrease in fraction of impulse energy absorbed versus amount of energy accumulated – reinforcement of the material under mechanical loadings has not been taken into account.
- volume loss of the material proceeds by extraction of debris until the whole layer is removed.

Two parameters of the probability function used in quantification procedure may hold physical meanings as: (1) value of impulse energy absorbed in element impinged. The process of energy absorption goes down with volume deformation of the material or cycle deformation specified by hysteresis. Cracking under external loading is preceded by generation the critical conditions, since external sources energy is transferred into surface energy of crevices. An increase in microcracks density is driven by subsequent impulses until the extraction of a debris occurs. It is linked to high rate of the loading force cycles and fatigue nature of the process and may be inferred from observation: the higher rate of the force action, the higher probability of micro-crack multiplication [46]. Summing up, fracture of solid proceeds by nucleation of cracks on the surface or generation micro-cracks in deeper layers, indispensable for creation the critical cracks. (2) value of energy threshold level for crack inception within the element. Having knowledge that crack inception depends on favourable local stress conditions the threshold level should be took as statistical parameter – an expected value for respective statistical distribution.

There could be found some conformities between the absorption of cavitation impulse energy absorption and transfer of and excitation energy transfer from donors to acceptors in multimolecular systems, modelled determined by Förster [47]. Fluorescence quantum yield depends on the efficiency of delivering the energy to donors and acceptors being the function of probability mass function of energy transfer. The latter depends on temporal densities of donors and acceptors within controlled number of the molecules [48,49]. As a consequence of accepting the conformities between mechanisms underlying the processes being compared the probability function of extraction of the unit of the material surface layer under cavitation loadings can be expressed by the following formula:

$$p(n) = \sqrt{\pi} \exp(n^2)\,(1 - \mathrm{erf}(0, n)) \tag{3}$$

where n stand for the average density of the energy trapping points within the layer. Thus the formula (3) is getting more exact if the thickness of the layer is being decreased. Attaining the value $p(n)=1$ means the layer is removed in total. It happens, if n is equal about 6 in formula (3). The average density of the energy (n) is a function of time.

In present paper considerations are performed within the exposition time interval confined by the condition: $n<6$. It approximately equals the incubation time of the erosion.

In present paper n was arbitrarily defined by two parameters w and s:

$$n = 6\left(\frac{t}{s}\right)^{w} \tag{4}$$

where w and s play the role of computation parameters. Parameter w is dimensionless. Parameter s is to be expressed in time units (in minutes).

<u>Model based on the Weibull statistical distribution</u>

It was assumed that erosion characteristics up to the maximum rate of the material volume loss follows the Weibull probability function integrated in the time domain. Calibrating adjustment is done by multiplying it by coefficient proportional to the loading intensity value. This approach leads to the formula, which satisfy the above assumption:

$$\delta(t) = \gamma \int_0^t \left(1 - \exp\left[-\left(\frac{\tau}{\alpha}\right)^{\beta}\right]\right) d\tau \tag{5}$$

Symbols in above formula denotes:
$t,\ \tau -$ time, where unit of measure was 100 min,
$\delta -$ mean depth of erosion, mm. Volume loss of the material $V(t)$ is than determined by multiplying the δ by the area of the material subjected to the loading,
$\gamma -$ coefficient, which depends on the energy delivered to the layer. It is evaluated as the product of constant coefficient equal to 2 mm³/J ×loading intensity W/mm²,
$\alpha -$ scale parameter being determined from formula (8),
$\beta -$ shape parameter, being determined from formula (9).

Parameter β is dimensionless, while parameter α is to be expressed in units of time, min.

Two calculation parameters used in quantification procedure may hold a physical meanings as a reciprocal of the fraction of impulse energy absorbed in element impinged (α) and () an energy threshold level for crack inception within the element (β).

Other implicit assumptions for building the formula were:
- mass loss rate during the process is driven by the value of cavitation loading and strength parameters of the material;

- mass loss rate during the process is proportional to average intensity of cavitation loading;
- target material and space distribution of the impulses are regarded statistically homogenous;
- parameters in the formula (5) are independent and are assumed constant for given material. Under that simplification their particular values could be determined from the given erosion curve;
- simplification is implicit: decrease in energy absorption versus amount of energy accumulated in element, i.e. reinforcement of the material under mechanical loadings is omitted.

3.2. Experimental data for recovering the values of parameters employed in the models

Functional relationships between calculation parameters and the strength parameters of the materials have been derived by completing procedure of adjusting the computed erosion curves to the experimental data for the vast diversity of the cases and subsequently revealing the existing correlations. Results obtained from both the International Cavitation Erosion Test program as well as the own experiments carried out at the rotating disk set-up supplied necessary experimental data.

Experimental data used in inferring the formulas for w and s parameters (Formulas (6) and (7)) were the results of the own experiments carried out at the rotating disk set-up at the Institute of Fluid Flow Machinery. Verification of the method based on probability function (3) have been carried out using the results of the International Cavitation Erosion Test. Conversely, experimental data used in inferring the formulas for α and β parameters (Formulas (8) and (9)) derived from the results of International Cavitation Erosion Test, whereas verification of the method based on probability function (5) have been carried out using the results of the own experiments.

<u>Results of the own experiments completed with the rotating disk device used</u>

Experimental tests have been conducted with the use of the rotating disk facility in The Szewalski Institute of Fluid Flow Machinery Polish Academy of Sciences in Gdańsk. Detailed description of the device has been presented in [50]. Disk with cylindrical cavitation inducers distributed along perimeter (Fig. 1) is submerged in the liquid and rotates. Fragment of the disk view exploded along the section through the centres of the inducers and specimens is presented in Figure 2, in which the dimensions of geometrical configuration required to determination of fluid-flow conditions are depicted. The latter are favourable for

generation of cavitation regions within the pulsating vortices. Cavitation number for the case was about 0.015. Rapid implosions of the bubbles occur in the zone more distant to the inceptor. Resultant micro-jets or shock waves generated mainly due to collective phenomena within cavitation zone exert forces on the solid wall thus embody the process of material erosion. Samples for investigations are positioned so that to be exposed to cavitation loadings. Hydraulic circuit containing pressure vessel with vacuum cushion serves for forcing the water circulation and maintaining a desired pressure inside the chamber. Basic operating parameters of the device were as follow:

- rotational velocity of the disk: 2950 rpm,
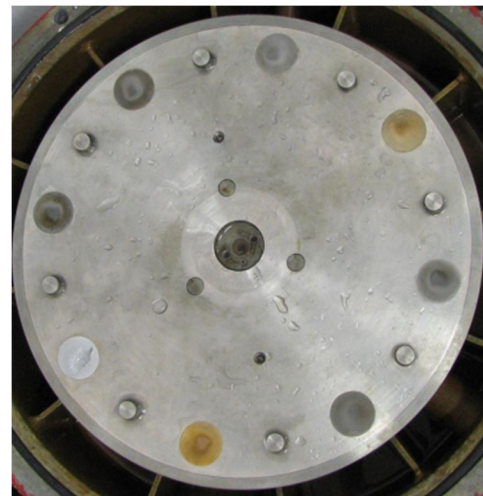- pressure in the chamber: 160 hPa.

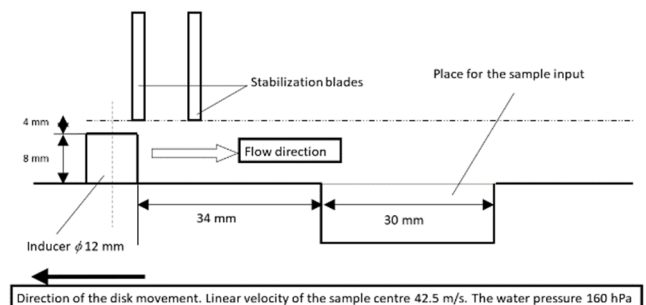Fig. 1. General view of the disk with inducers and samples distributed at the perimeter

Fig. 2. Fragment of the disk view exploded along the section through the centres of the inducers and specimens

Temperature of the liquid medium is stabilized within 18°C to 21°C. Average value of density of energy flux was computed in line with Steller fractional method and

approximately equalled 167 W/cm² [51]. Exposition of samples to cavitation lasted up to 360 min, but for the sake of present investigations only volume losses in the initial period of the erosion have been regarded (Figs 3-9).
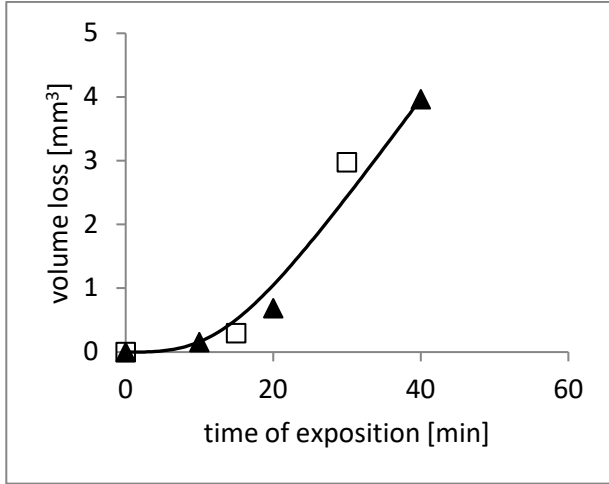

Fig. 3. Experimental results of the erosion of the CuZn40Pb2 (MO58) brass (discernible points) and theoretical curve determined by simulating procedures (continuous line)
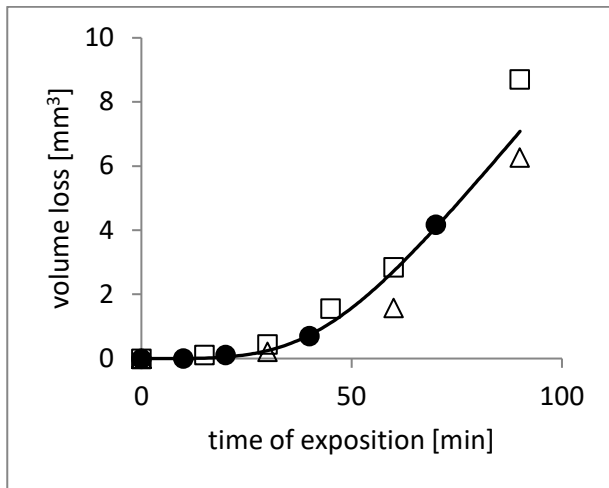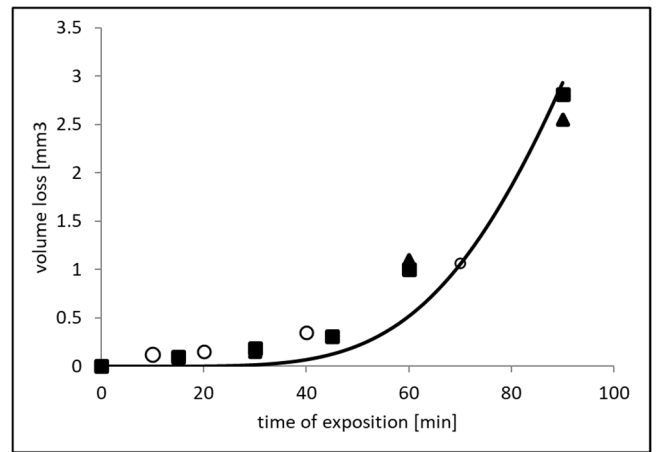

Fig. 4. Experimental results of the erosion of the X6CrNiTi18-10 (1H18N9T) steel (discernible points) and theoretical curve determined by simulating procedures (continuous line)

Cavitation erosion of seven materials detected experimentally and corresponding cavitation erosion curves determined numerically on base of the model presented in Section "Model inspired by Forster energy migration theory" are shown in Figures 3-9. The materials chosen

were: yellow brass, aluminium magnesium alloy: hardened and not hardened, chromium non-resistant steel rolled without heat processing and after heat treatment, acid resistant steel and two-phase corrosion resistant steel depicted according to PN-EN (and old Polish Norms – in brackets) correspondingly: CuZn40Pb2 (MO58), CuAl10Fe3Mn2 (BA1032), CuAl10Fe3Mn2 (BA1032) hardened and tempered, X20Cr13 (2H13), X20Cr13 (2H13) hardened and tempered, X6CrNiTi18-10 (1H18N9T), X2CrNiMoN22-5-3 (Duplex 2205) with strength parameters presented in Table 1.

Fig. 5. Experimental results of the erosion of the CuAl10Fe3Mn2 (BA1032) bronze (discernible points) and theoretical curve determined by computation (continuous line)
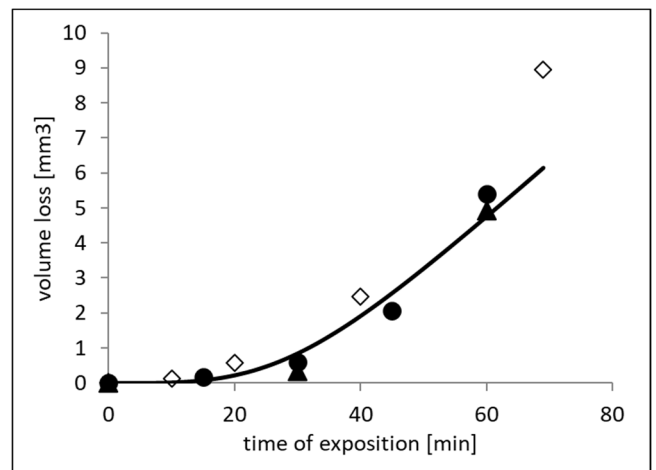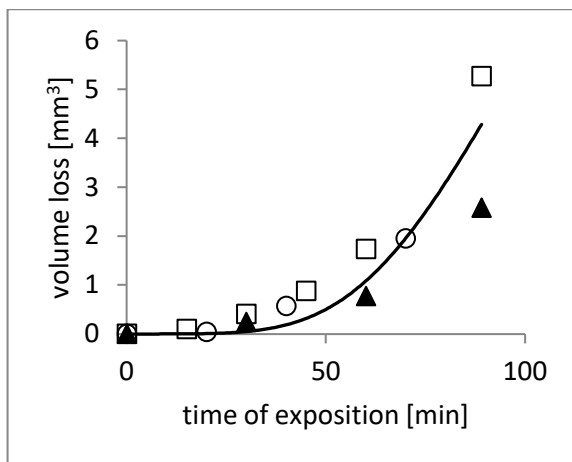

Fig. 6. Experimental results of the erosion of the X20Cr13 (2H13) steel (discernible points) and theoretical curve determined by computation (continuous line)
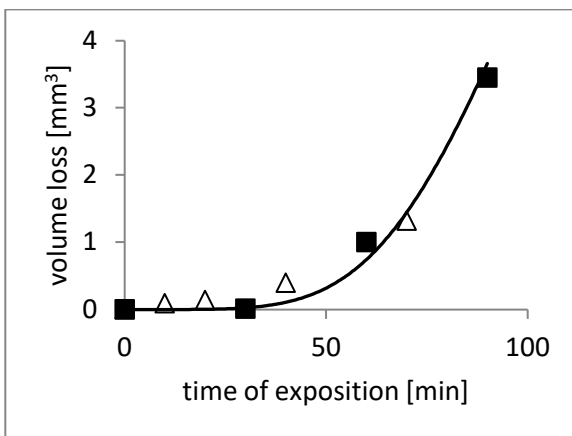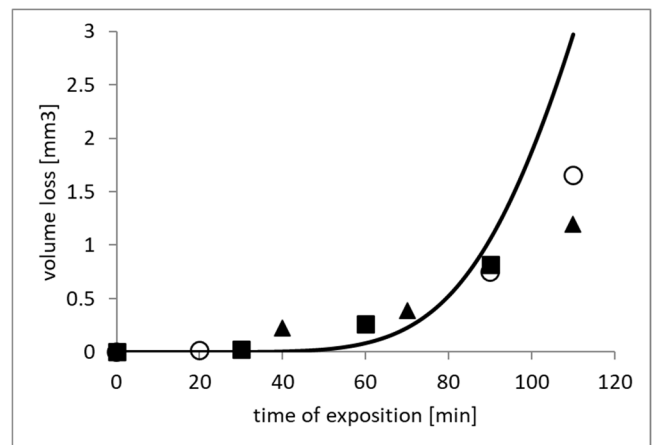
Table 1.
Mechanical properties of the material tested

	Density, g/cm^3	Vickers hardness, HV10	Tensile strength, R_m, MPa	Yield strength, R_e, MPa	Fatigue tensile strength, S_f, MPa	Hardening exponent, -	Young 's modulus, E, GPa
CuZn40Pb2 (MO58)	8.4	119	457	165	140	0.35	96
X6CrNiTi18-10 (1H18N9T)	7.88	191	605	225	465	0.73	200
X20Cr13 (2H13)	7.75	192	863	432	271	0.49	200
X20Cr13 (2H13) hardened and tempered	7.75	244	1116	658	275	0.47	200
X2CrNiMoN22-5-3 (Duplex 2205)	7.82	310	763	496	530	0.52	200
CuAl10Fe3Mn2 (BA1032)	7.51	202	730	240	255	0.57	115
CuAl10Fe3Mn2 (BA1032) hardened and tempered	7.51	243	793	415	355	0.7	115

Fig. 7. Experimental results of the erosion of the X20Cr13 (2H13) hardened and tempered steel (discernible points) and theoretical curve determined by computation (continuous line)

Fig. 9. Experimental results of the erosion of the CuAl10Fe3Mn2 (BA1032) hardened and tempered bronze (discernible points) and theoretical curve determined by computation (continuous line)

Results of the International Cavitation Erosion Test used

Results obtained at the International Cavitation Erosion Test (ICET) program are available in [1]. In present work erosion characteristics of four materials (brass M63: Zn 32.6, Cu rest; Armco iron E04: C 0.035, Mn 0.1, Si 0.01, P 0.026, S 0.035, Fe rest; carbon steel 45: C 0.43, Mn 0.63, Si 0.26, P 0.03, S 0.033, Fe rest; and 1H18N9T acid resistant steel: C 0.08, Mn 1.37, Si 0.55, P 0.03, S 0.01, Cr 17.6, Ni 9.4, Ti 0.6, Fe rest) tested at nine laboratories (Tab. 2) have been employed as the source of the experimental data. Strength parameters of the materials tested were put together in the Table 3.

A representative experimental results and corresponding cavitation erosion curve determined numerically on base of the model presented in Section "Model based on the Weibull statistical distribution" are shown in Figure 10.

Fig. 8. Experimental results of the erosion of the X2CrNiMoN22-5-3 (Duplex 2205) steel (discernible points) and theoretical curve (continuous line)

Table 2.
Chosen participants of the ICET [4]

Laboratory	Type of the test
China Ship Scientific Research Centre, Wuxi	Vibratory rig
CISE S.p.A., Milan	Vibratory rig
Fluid Control Research Institute, Palghat	Cavitating jet
Institute of Fluid-Flow Machinery, Pol. Ac. Sci., Gdansk	Vibratory rig
SIGMA Research Institute, Olomouc	Liquid jet
The City University, London	Cavitation tunnel
Tsinghua University, Beijing	Vibratory rig
University of Cape Town, Rondebosch	Vibratory rig
University of Hannover, Hannover	Cavitating jet

Table 3.
Strength parameters of some materials tested in ICET and employed in present work [24]

Parameter/Material designation	Symbol	M63	E04	Steel 45	1H18N9T
Density, kg/m^3	ρ	8.43	7.85	7.87	7.88
Vickers hardness, HV$_{10}$	HV	80.9	108.4	192.8	191
Tensile strength, MPa	R_m	352	328	721	605
Yield strength, MPa	R_e	117	263	419	225
Fatigue strength, MPa	S_f	140	199	278.5	485
Elongation to break, %	$\%$	65	40.5	22	52
Hardening exponent, -	n	0.35	0.23	0.21	0.54
Young's modulus E, GPa	E	99	210	210	200
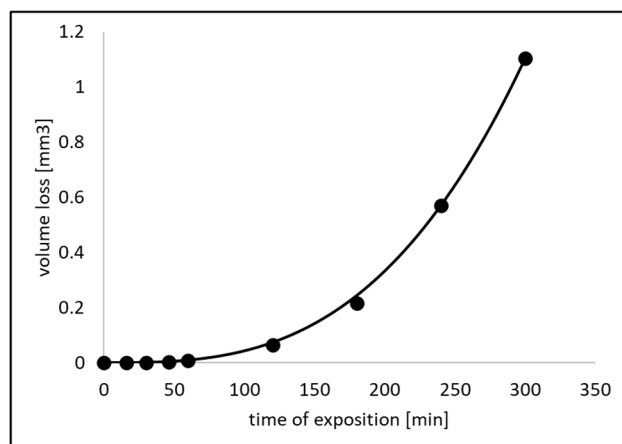
Fig. 10. Experimental and theoretical values of volume loss of Armco iron E04 tested at the laboratory rig – cavitation tunnel in Fluid Control Research Institute. Approximate value of the loading intensity was 26.7 W/cm^2. Theoretical volume loss refer to the Weibull distribution parameters: $\alpha = 22$; $\beta = 1.98$. In that case the incubation time determined according to K. Steller definition equalled 180 min

3.3. Determining the relationships between model computational parameters and strength parameters of the material

Each material tested was featured by its mechanical properties, by assumption related unambiguously to the computation parameters. That led to phenomenological way for providing the parameters values: values of parameters w and s or α and β were derived by adjusting the computed erosion curve to experimental results. Approximation was carried out by selection of the parameters, which were gradually varied until the experimental points, i.e. volume loss of the material versus time of exposition were imposed with acceptable accuracy, according to the following routine: (1) Each set of experimentally measured volume losses, referring to define material and loading conditions has been approximated by the computed erosion curve. Herein proposed two alternative methods of determining the erosion curve were described in Sections "Model inspired by Forster energy migration theory" and "Model based on the Weibull statistical distribution". Adjustment has been

achieved by changing values of computation parameters. An example of such adjustment is presented in Figure 10. (2) Significant dispersion of experimental data forced the mean value have been taken. (3) Coupling separately the values of computational parameters to chosen measurable properties let the appropriate relationship to be defined.

The parameters obtained concern the particular experimental data and refer to defined loading conditions and material characteristics. Due to poor repeatability of experimental characteristics, the mean results should be taken of numerous experimental cases. Sets of calculation parameters taken of various materials eroded under same conditions can be referred to strength parameters of the materials enabling the adequate relationships to establish.

Values of parameters w and s have been derived from Figures 3-9. Thus, the functional dependences of w and s on the strength parameters product $((Sf/E+Rm/E)*HV)$ were able to be obtained in graphical form (Figs 11 and 12).
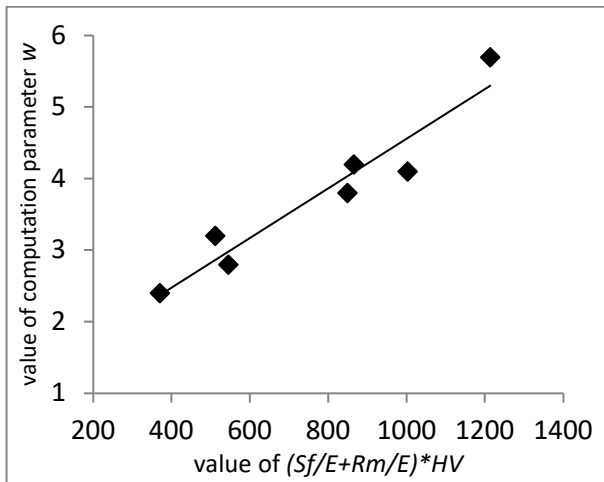
Fig. 11. Graph presentation of the w value vs. the HV, Rm, E and Sf parameters product. Continuous trend line is depicted

Functional relationships between calculation parameters w and s and the strength parameters of the materials are as follows:

$$w = 0.0035 \cdot \frac{HV \cdot (S_f + R_m)}{E} + 1.0836 \tag{6}$$

$$s = 87.137 \cdot ln\left[\frac{HV \cdot (S_f + R_m)}{E}\right] - 463.48 \tag{7}$$

It follows from the measurement results that monotonic, unambiguous relationships have been obtained for same experimental conditions.

Values of parameters α and β have been derived by approximating the ICET results. After the sets of calculation parameters (α and β) had been referred to strength

parameters of the materials, the adequate relationships have been obtained. The ultimate functional dependences of α and β on the strength parameters were presented in graphical form in Figures 13-15.
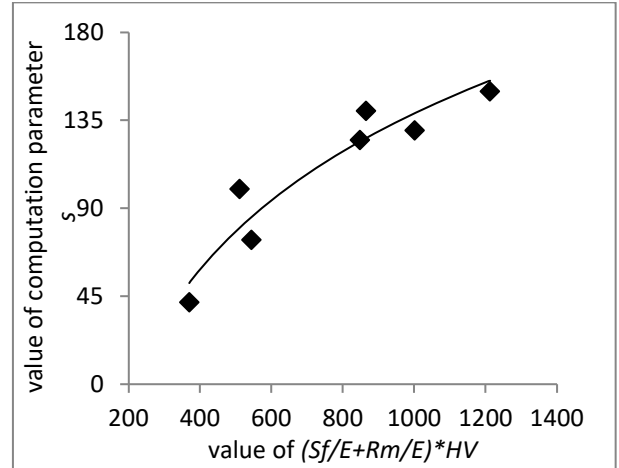

Fig. 12. Graph presentation of the s value vs. the HV, Rm, E and Sf parameters product. Continuous trend line is depicted
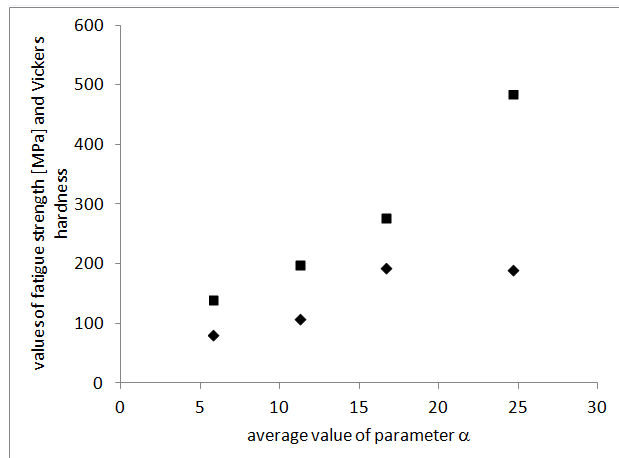

Fig. 13. Relationships between parameter α and measurable parameters: fatigue strength (square) and hardness (diverted square)

Computation rules for calculation parameters α and β are disclosed in following formulas

$$\beta = 0.2574 \, ln(x) + 1.8 \tag{8}$$
$$\alpha = 15.22 ln(S_f) - 69.3 \tag{9}$$

where

$$x = 0.3 \cdot \left(\frac{S_f}{R_m}\right) \cdot \left(\frac{HV}{\%}\right)^{n^{0,4}}$$

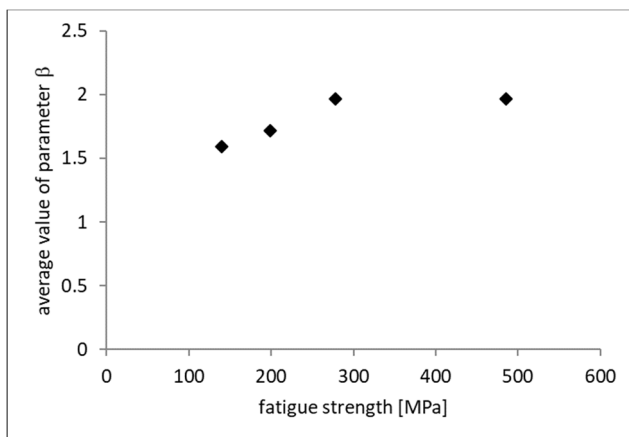Designations used in formulas (6), (7), (8) and (9) were explained in Table 3.

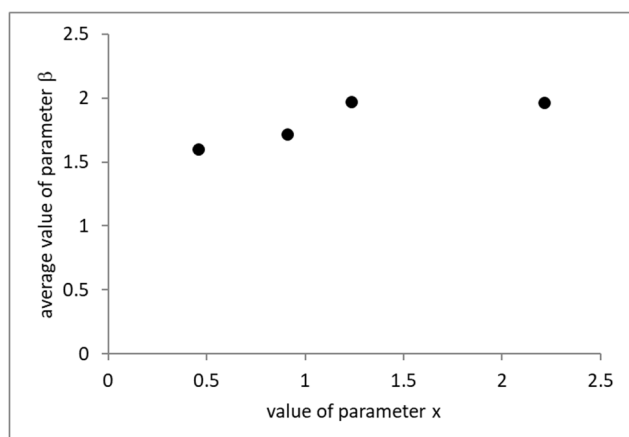Fig. 14. Relationships between parameter β and measurable parameter: fatigue strength

Fig. 15. Relationships between parameter β and function x of measurable parameters
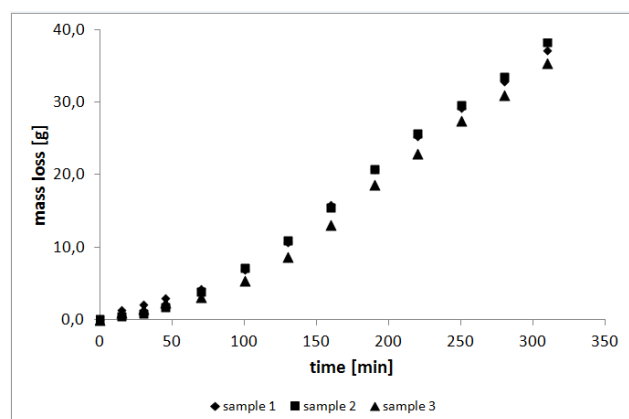

Fig. 16. Experimental results of the erosion of Armco iron (E04) processed at the CSSRC, Wuxi laboratory within the ICET program

4. Uncertainties in cavitation erosion prediction

Analysis of the process randomness as well as determination of the possible uncertainties and errors due to unrepeatability of the experimental results is an important issue connecting investigations on the cavitation erosion. In order to be conscious of the possible inaccuracy in predicting the erosion through the method with the values of w and s or α and β employed, some assessments of the statistical unrepeatability of the source experimental results obtained at the same conditions have been done. The rough estimation of the reliability of the ICET results has been completed due to wide range of the accessible data. Dispersion of the specified material volume loss measured under the same loading conditions has been considered. The deviations, i.e. the difference between given volume loss and average volume loss divided by average volume loss stand for the random values. Each particular deviation have been determined for the particular set of the experimental curves obtained at the same laboratory rig for the same material. The deviations expressed in percentages have been found at the time of exposition referring to the maximum rate of the volume loss. As an example, in Figure 16 the maximum erosion rate is at about 160 min of exposition. At that point the ultimate difference of the mass loss for three samples equalled 2.6 mg (15.8-13.3 mg). In order to determine the probability functions of various deviations, the following procedure has been applied: (1) four ranges of the deviation values has been distinguished and the number of cases relating each range has been determined. The number of cases for given material results from computations over all families of experimental curves for all participant laboratories according the above presented method. Same, the number of cases for given range of loadings results from computations over all families of experimental curves for respective laboratories according the above presented method; (2) by dividing the particular numbers to the total number of deviation cases the corresponding probabilities have been obtained, thus enabling the appropriate probability function to be accomplished. Histograms of probabilities referred to four materials investigated were presented in Figs 17-20.

Probabilities of the occurrence of deviations of various particular experimental results from the average value for two distinguished ranges of loading intensities have been presented in Figures 21 and 22. The ranges of the loading intensities have been assumed as follows:
(1) intensities below 2.5 W/cm² (16 sets of data referring to 5 laboratories and various materials have been used in considerations);

(2) intensities over 2.5 W/cm^2 (16 sets of data referring to 4 laboratories and various materials have been used in considerations).
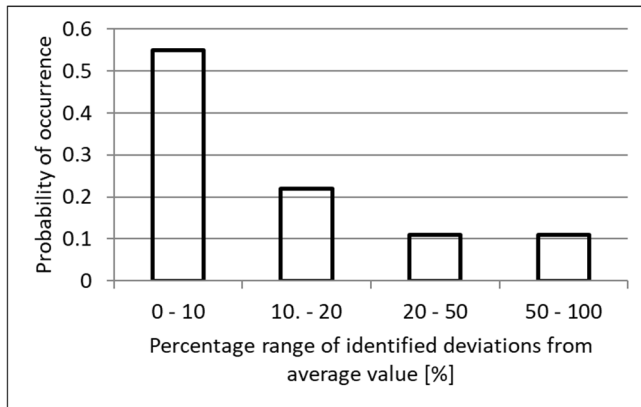

Fig. 17. Probability of occurrence of various ranges deviations. Data refer to the EO4 iron
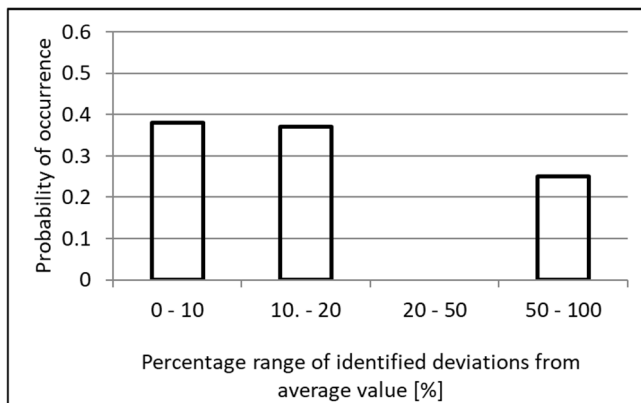

Fig. 18. Probability of occurrence of various ranges deviations. Data refer to the steel 45
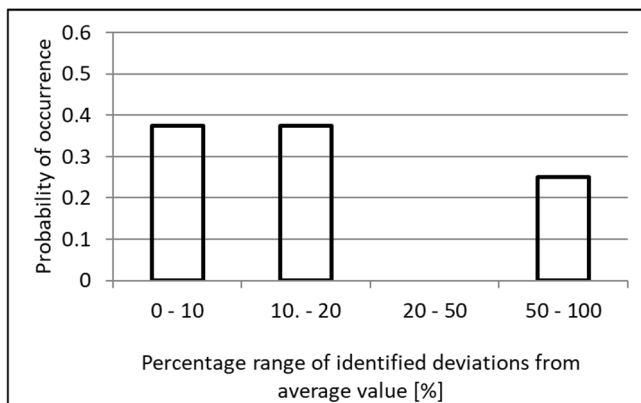

Fig. 19. Probability of occurrence of various ranges deviations. Data refer to the steel 1H18N9T
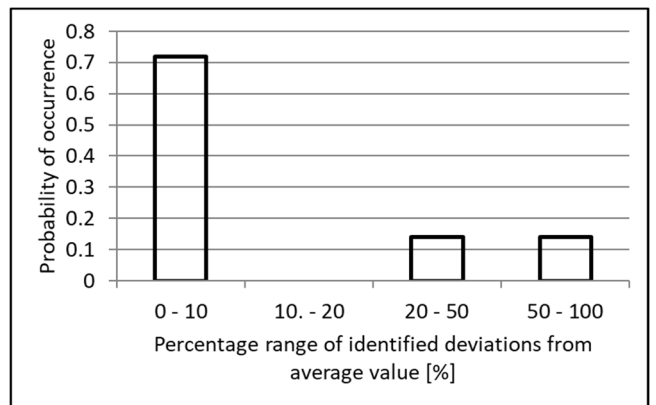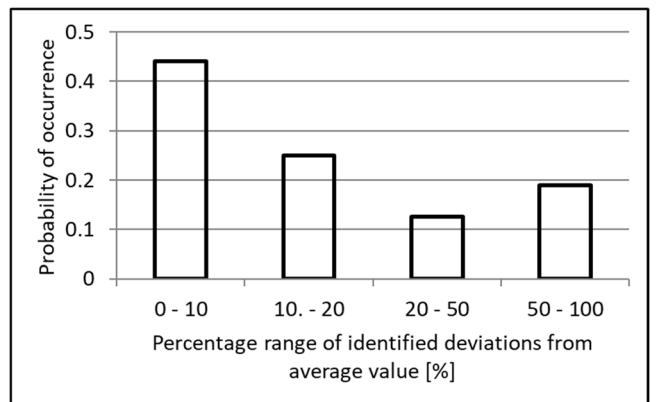

Fig. 20. Probability of occurrence of various ranges deviations. Data refer to the brass 63

Fig. 21. Probability of occurrence of various ranges deviations. Data refer to the loading intensities below 2.5 W/cm^2
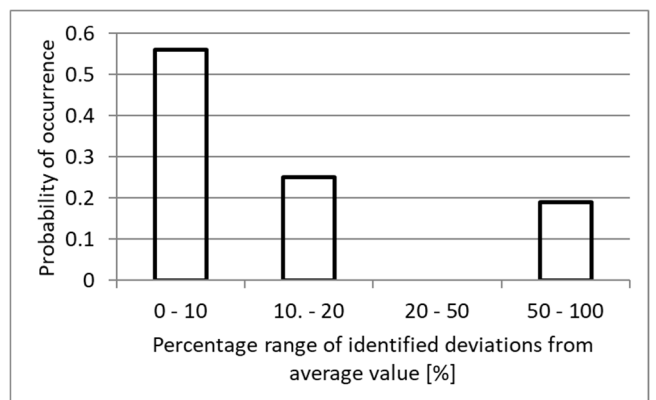

Fig. 22. Probability of occurrence of various ranges deviations. Data refer to the loading intensities over 2.5 W/cm^2

5. Verification of the method

In order to validate the method the control calculations have been carried out for the cavitation erosion cases obtained under International Cavitation Erosion Test (if the model based on the Forster theory was used) and the own results obtained at the rotating disk rig (if the model based on the Weibull distribution was used).

5.1. Verification of the method if the model based on the Forster theory is used

Particular results obtained at the vibratory rigs in China Ship Scientific Research Center (CSSRC) and Hiroshima University (HIRO) laboratories are presented in Figures 23 and 24. Average values of density of energy flux determined by Steller fractional method were approximately 90.6 W/cm^2 and 101.3 W/cm^2 [51]. Corresponding theoretical curves (continuous lines), resulting from model calculations are displayed.
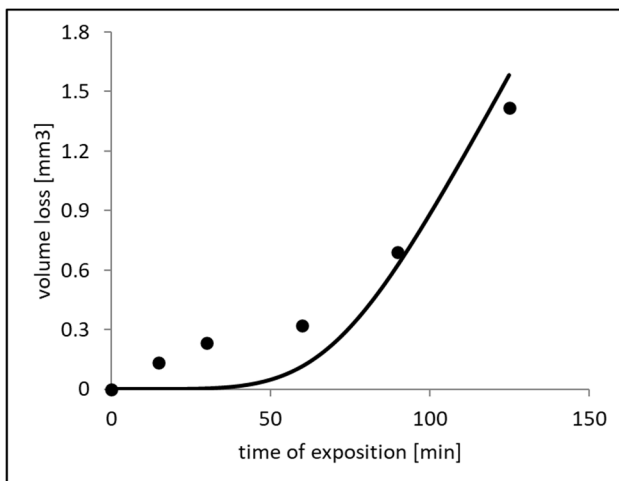

Fig. 23. Cavitation erosion of the 45 steel performed at the vibratory rig in CSSRC Lab. (discernible points) and theoretical curve determined by computation (continuous line)

5.2. Verification of the method if the model based on the Weibull distribution is used

This time the experimental results obtained at the rotating disk rig in the Szewalski Institute of Fluid Flow Machinery Polish Academy of Sciences in Gdańsk were used to verify the soundness of the method. The volume losses of the stainless chromium steel X20Cr13 (2H13),

acid-resistant stainless steel X6CrNiTi18-10 (1H18N9T) and two-phase steel X2CrNiMoN22-5-3 (Duplex 2205) in the initial stage of the erosion have been compared to the computation results. Experimental results (discernible points) and corresponding theoretical curves (continuous lines) resulting from model calculations are displayed in Figures 25-26.
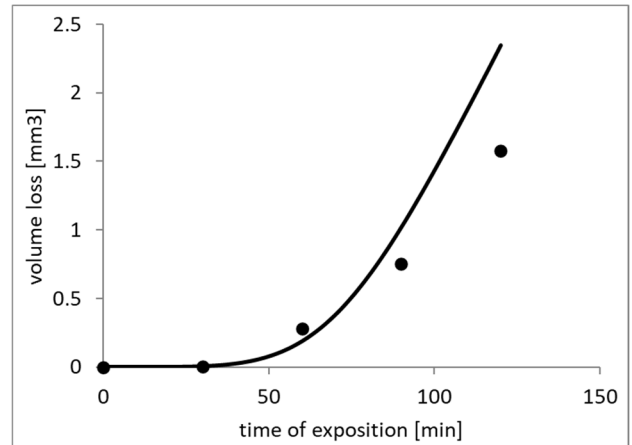

Fig. 24. Cavitation erosion of the 45 steel performed at the vibratory rig in HIRO Lab. (discernible points) and theoretical curve determined by computation (continuous line)
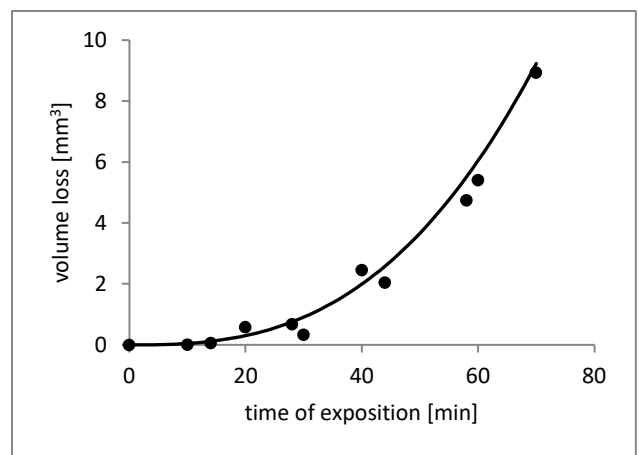

Fig. 25. Cavitation erosion performance of the steel X20Cr13 (2H13). The results of the three series of experimental runs (discernible points) and the curve determined by applying the formulas (5), (8), and (9) (continuous line)
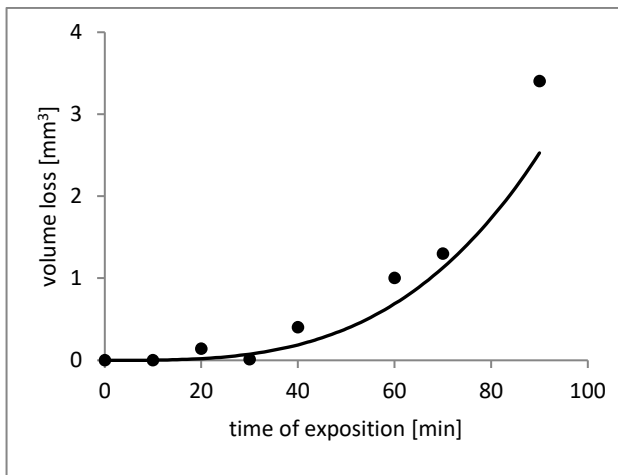
Fig. 26. Cavitation erosion performance of the steel Duplex 2205. The results of the three series of experimental runs (discernible points) and the curve determined by applying the formulas (5), (8), and (9) (continuous line)
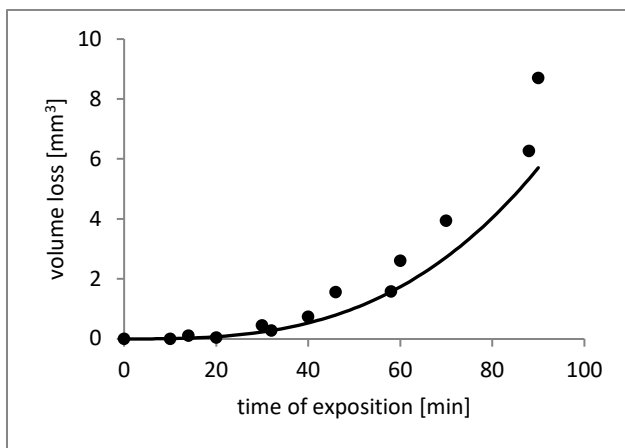

Fig. 26. Cavitation erosion performance of the steel X2CrNiMoN22-5-3 (Duplex 2205). The results of the three series of experimental runs (discernible points) and the curve determined by applying the formulas (5), (8), (9) (continuous line)

6. Discussion and primary inferences. Possible drawbacks of the method

Basic charge of the method include determination of the erosion performance in the initial period of the process. Consistency between the erosion curves derived using the methodology described and the experimental data, representatively shown in Figures 23-26 is acceptable in most cases. However, in some cases major discrepancies have been identified. The discrepancies were primarily caused by: (a) insufficiently precise formulas for computational parameters – relationships (6)-(8), i.e. computational parameters derived from the formulas may deviate from the average computational parameters determined by adjusting the experimental results. It may be assumed that better relevance of the prediction would be achieved if the more precise and unambiguous relationships were obtained, e.g. by employing more experimental results to derive them; (b) the lack of consistency of the experimental data providing the basis for determining the calculation parameters. Calculation parameters derived by adjusting the experimentally determined volume loss of the same material may be noticeably different due to randomness of the loading conditions and material properties. The essential source of that deficiency is very limited number of experimental runs to establish the formulas (6)-(8); (c) model imperfections – an assumption on the independence of the calculation parameters on the loadings, which implies that calculation parameters referring to various loadings may be considerably different. Inaccuracy in measurement results and uncertainty linked to stochastic nature of the process may be reduced by employing more experimental characteristics as well as employing more materials of different properties.

Nevertheless, the results indicate there are obvious relationships between the fatigue strength of the material and the calculation parameters α and β or w and s (accordingly Figs 11-15) and identifiable relationship between the hardness of the material and the calculation parameter α (Figs 11, 12, 13, and 15). As a side note, the results confirm the conviction that unambiguous correlation between the fatigue strength of the material and its erosion performance exists. Therefore, the formula (1) with the relations (3), (4), (6), and (7) or the formula (5) supplemented with the relations (8) and (9) enable to predict the extent of material damage under the defined loadings using only strength parameters values. However, various simplifications may influence on the method soundness. For example there is not known the effect of the discount the mechanical hardening of the material, despite the hardening exponent has been taken into account in formula (8). Moreover, one may expect the possible deviations from real effectiveness of the erosion due to the nonstationary nature of the cavitation impingements action – behaviour of materials under very high strain rates (10^{-4}-10^{-6} s^{-1} [52]) differs from that occurring in quasi stable conditions. Omitting the differences in changes of micromechanical properties or effectiveness of possible phase transformations under cavitation loading may be meaningful. It is supposed

the deficiency of the present approach. Nevertheless, an assumption on dependence of the material disintegration on the temporal density of the hypothetical energy trapping points may allow help to address the problem and the aquiline dependences of parameters w and s on the material strength parameters (Figs 11, 12) would help to reduce the ambiguities of the results of computations.

Despite the experimental data employed in the analysis refer to the erosion performed at the facilities of different loadings (the ICET results), the functions in Figs 13-15 are smooth, which may provide proof of their independence on the loadings. That may be the case of linear dependence of the volume loss on the loading value. Analysis made over the ICET results revealed compelling relationship between the divergence of the experimentally detected material volume losses and its erosion resistance – thus divergence in case of the steels 45 and 1H18N9T substantially exceeds the divergence in case of the less resistant materials: technical iron E04 and brass 63. It is worth to be mentioned that characteristics of the distributions for steels 45 and 1H18N9T are the same and the characteristics of the distributions for iron E04 and brass 63 are also close enough. It is still not documented persuasively statement, but assumption on the influence of the erosion resistance on the repeatability of the erosion performance of the material in the stationary conditions seems to be reasonable. Moreover, it can be inferred that divergence of the material volume losses is perhaps independent on its physical characteristics.

Bearing in mind that dependencies elicited in Figures 11-15 have been obtained by adjusting the theoretical curve to the experimental results up to the exposition time referring to the maximum rate of the erosion, the usability of the method is confined to initial period of the damage.

References

[1] J. Steller, B.G. Gireń, International Cavitation Erosion Test Final Report, Reports of The Szewalski Institute of Fluid Flow Machinery Polish Academy of Sciences, Gdańsk, 560/1519/2015.

[2] A. Antonini, A. Giadrossi, Turbine behavior under cavitation conditions, International Water Power & Dam Construction 33 (1981) 25-28.

[3] L. Bellet, E. Laperrousaz, J.M. Dorey, P. Bourdon, M. Farhat, R. Simoneau, F. Avellan, P. Dupont, M. Couston, Cavitation erosion prediction on Francis turbines, International Journal on Hydropower and Dams 4/3 (1997) 56-58.

[4] J. Steller, International Cavitation Erosion Test and quantitative assessment of material resistance to cavitation, Wear 233-235 (1999) 51-64. DOI: https://doi.org/10.1016/S0043-1648(99)00195-7

[5] J. Steller (Test coordinator), International Cavitation Erosion Test, Experimental rigs, data available: 13.10.2016 at http://www.imp.gda.pl/icet/

[6] R. Hickling, M.S. Plesset, Collapse and rebound of a spherical bubble in water, Physics of Fluids 7/7 (1964) 7-14. DOI: https://doi.org/10.1063/1.1711058

[7] A. Thiruvengadam, S. Waring, Mechanical Properties of Metals and their Cavitation Damage Resistance, Journal of Ship Research 10 (1966) 1-9.

[8] A. Karimi, L.J. Martin, Cavitation Erosion of Materials, International Materials Reviews 31/1 (1986) 1-26.

[9] R.H. Richman, W.P. McNaughton, Correlation of cavitation erosion behaviour with mechanical properties of metals, Wear 140/1 (1990) 63-82. DOI: https://doi.org/10.1016/0043-1648(90)90122-Q

[10] B.G. Gireń, M. Szkodo, J. Steller, The Influence of Residual Stresses on Cavitation Resistance of Metals — an analysis based on investigations of metals remelted by laser beam and optical discharge plasma, Wear 233-235 (1999) 86-92.
DOI: https://doi.org/10.1016/S0043-1648(99)00200-8

[11] B.G. Gireń, Material Proprieties Essential for Cavitation Erosion of Laser Produced Surface Alloys, Journal of Materials Science 39 (2004) 295-297. DOI: https://doi.org/10.1023/B:JMSC.0000007759.44511.c3

[12] S. Hattori, R. Ishikura, Revision of Cavitation Erosion Database and Analysis of Stainless Steel Data, Wear 268/1-2 (2010) 109-116.
DOI: https://doi.org/10.1016/j.wear.2009.07.005

[13] F.J. Heymann, On the Time Dependence of the Rate of Erosion Due to Impingement or Cavitation, Erosion by Cavitation or Impingement, Erosion by Cavitation or Impingement 408 (1967) 70-110. DOI: https://doi.org/10.1520/STP46046S

[14] E.H.R. Wade, C.M. Preece, Cavitation erosion of iron and steel, Metallurgical Transactions A: Physical Metallurgy and Materials Science 9 (1978) 1299-1310. DOI: https://doi.org/10.1007/BF02652254

[15] V.P. Morozov, Cavitation Noise as a Train of Sound Pulses Generated at Random Times, Soviet Physics-Acoustic 14/3 (1969) 361-365.

[16] J. Kalestrup Kristensen, I. Hansson, K.A. Morch, A simple model for cavitation erosion of metals, Journal of Physics D: Applied Physics 11/6 (1978) 899-912. DOI: https://doi.org/10.1088/0022-3727/11/6/009

[17] F.G. Hammit, M.K. De, Cavitation Damage Prediction, Wear 52/2 (1979) 243-262.
DOI: https://doi.org/10.1016/0043-1648(79)90066-8

[18] A. Karimi, W.R. Leo, Phenomenological Model for Cavitation Erosion Rate Computation, Materials Science and Engineering 95 (1987) 1-14. DOI: https://doi.org/10.1016/0025-5416(87)90493-9

[19] F. Pereira, F. Avellan, P. Dupont, Prediction of cavitation erosion – an energy approach, Journal of Fluid Engineering, Transactions of ASME 120/4 (1998) 719-727.
DOI: https://doi.org/10.1115/1.2820729

[20] N. Berchiche, J-P. Franc, J-M. Michel, A model for the prediction of the erosion of ductile materials by cavitation, Comptes Rendus del Academie des Sciences Series IIB – Mechanics-Physics-Astronomy 328/4 (2000) 305-310.
DOI: https://doi.org/10.1016/S1287-4620(00)00134-4

[21] N. Berchiche, J-P. Franc, J-M. Michel, A Cavitation Erosion Model for Ductile materials, Journal of Fluids Engineering 124/3 (2002) 601-606.
DOI: https://doi.org/10.1115/1.1486474

[22] M. Dular, B. Stoffel, B. Sirok, Development of a Cavitation Erosion Model, Wear 261/5-6 (2006) 642-655. DOI: https://doi.org/10.1016/j.wear.2006.01.020

[23] B.G. Gireń, J. Steller, Random multistage input and energy partition approach to the description of cavitation erosion process, Stochastic Environmental Research and Risk Assessment 23 (2009) 263-273.
DOI: https://doi.org/10.1007/s00477-007-0200-8

[24] B.G. Gireń, J. Frączak, Phenomenological prediction tool for cavitation erosion fed with the International Cavitation Erosion Test results, Wear 364-365 (2016) 1-9. DOI: https://doi.org/10.1016/j.wear.2016.06.005

[25] A. Peters, H. Sagar, U. Lantermann, O. el Moctar, Numerical modelling and prediction of cavitation erosion, Wear 338-339 (2015) 189-201. DOI: https://doi.org/10.1016/j.wear.2015.06.009

[26] P. Veerabhadra Rao, D.H. Buckley, M. Matsumura, A unified relation for cavitation erosion, International Journal of Mechanical Sciences 26/5 (1984) 325-335.
DOI: https://doi.org/10.1016/0020-7403(84)90060-2

[27] R. Fortes-Patella, J.L. Reboud, The new approach to evaluate the cavitation erosion power, Journal of Fluid Engineering 120/2 (1998) 335-344. DOI: https://doi.org/10.1115/1.2820653

[28] P.B. Robinson, J.R. Blake, I. Kodama, A. Shima, Y. Tomita, Interaction of cavitation bubbles with a free surface, Journal of Applied Physics 89/12 (2001) 8225-8237. DOI: https://doi.org/10.1063/1.1368163

[29] D.R. Stinebring, J.W. Holl, R.E.A. Arndt, Two Aspects of Cavitation Damage in the Incubation Zone: Scaling By Energy Considerations and Leading Edge Damage, Journal of Fluid Engineering 102/4 (1980) 481-485.
DOI: https://doi.org/10.1115/1.3240729

[30] P. Veerabhadra Rao, D.H. Buckley, Cavitation Erosion Size Scale Effects, Wear 96/3 (1984) 239-253. DOI: https://doi.org/10.1016/0043-1648(84)90039-5

[31] Y. Lecoffre, J. Marcoz, J.P. Franc, J.M. Michel, Tentative procedure for scaling cavitation damage, Proceedings of the International Symposium on Cavitation in Hydraulic Structures and Turbomachinery, Albuquerque, USA, 1985.

[32] P. Veerabhadra Rao, D.H. Buckley, Unified Empirical Relations for Cavitation and Liquid Impingement Erosion Processes, Wear 120/3 (1987) 253-288. DOI: https://doi.org/10.1016/0043-1648(87)90022-6

[33] Y. Lecoffre, Cavitation Erosion, Hydrodynamic Scaling Laws, Practical Method of Long Term Damage Prediction, Proceedings of the International Symposium on Cavitation, CAV'95, Deauville, France, 1995.

[34] J-K. Choi, A. Jayaprakash, G.L. Chahine, Scaling of cavitation erosion progression with cavitation intensity and cavitation source, Wear 278-279 (2012) 53-61.
DOI: https://doi.org/10.1016/j.wear.2012.01.008

[35] M. Petkovsek, M. Dular, Simultaneous observation of cavitation structures and cavitation erosion, Wear 300/1-2 (2013) 55-64.
DOI: https://doi.org/10.1016/j.wear.2013.01.106

[36] B.G. Gireń, M. Noińska-Macińska, Cavitation erosion regimes – an attempt of deriving classification predictor, Transactions of the Institute of Fluid Flow Machinery 132 (2016) 1-15.

[37] O.I. Balyts'kyi, J. Chmiel, P. Krause, J. Niekrasz, M. Maciąg, Role of hydrogen in the cavitation fracture of 45 steel in lubricating media, Materials Science 45/5 (2009) 651-654.

[38] W. Bedkowski, G. Gasiak, C. Lachowicz, A. Lichtarowicz, T. Łagoda, E. Macha, Relations between cavitation erosion resistance of materials and their fatigue strength under random loading, Wear 230/2 (1999) 201-209. DOI: https://doi.org/10.1016/S0043-1648(99)00105-2

[39] Y. Iwai, T. Okada, S. Tanaka, A Study of Cavitation Bubble Collapse Pressures and Erosion part 2: Estimation of Erosion from the Distribution of Bubble Collapse Pressures, Wear 133/2 (1989) 233-243. DOI: https://doi.org/10.1016/0043-1648(89)90038-0

[40] C. Bojarski, J. Grabowska, L. Kułak, J. Kuśba, Investigations of the Excitation Energy Transport Mechanism in Donor-Acceptor Systems, Journal of Fluorescence 1 (1991) 183-191.
DOI: https://doi.org/10.1007/BF00865365

[41] H. Li, D. Wen, Z. Lu, Y. Wang, F. Deng, Identifying the Probability Distribution of Fatigue Life Using the

Maximum Entropy Principle, Entropy 18 (2016) 111. DOI: https://doi.org/10.3390/e18040111

[42] Y. Meged, Modelling of the initial stage in vibratory cavitation erosion tests by use of a Weibull distribution, Wear 253/9-10 (2002) 914-923.
DOI: https://doi.org/10.1016/S0043-1648(02)00037-6

[43] M. Szkodo, Mathematical description and evaluation of cavitation erosion resistance of materials, Journal of Materials Processing Technology 164-165 (2005) 1631-1636.
DOI: https://doi.org/10.1016/j.jmatprotec.2005.01.006

[44] A. Jayaprakash, J-K. Choi, G.L. Chahine, F. Martin, M. Donnelly, J-P. Franc, A. Karimi, Scaling study of cavitation pitting from cavitating jets and ultrasonic horns, Wear 296/1-2 (2012) 619-629. DOI: https://doi.org/10.1016/j.wear.2012.07.025

[45] S. Singh, J-K. Choi, G. Chahine, Characterization of cavitation fields from measured pressure signals of cavitating jets and ultrasonic horns, Journal of Fluids Engineering 135/9 (2013) 091302. DOI: https://doi.org/10.1115/1.4024263

[46] K. Tuncay, A. Park, P. Ortoleva, A forward model of three-dimensional fracture orientation and characteristics, Journal of Geophysical Research 105/B7 (2000) 16719-19735.
DOI: https://doi.org/10.1029/1999JB900443

[47] T. Förster, Experimentelle und theoretische Untersuchung des zwischenmolecularen Uebergangs von Electronenanregungsenergie, Zeitschrift Für Naturforschung 4A (1949) 321-327 (in German).

[48] R. Twardowski, J. Kuśba, C. Bojarski, Donor fluorescence decay in solid solution, Chemical Physics 64 (1982) 239-248. DOI: https://doi.org/10.1016/0301-0104(82)87090-0

[49] B.G. Gireń, Z. Polacki, The influence of excitation energy migration on excitation energy transfer, Journal of Photochemistry & Photobiology A: Chemistry 52/2 (1990) 321-326. DOI: https://doi.org/10.1016/1010-6030(90)80010-U

[50] B.G. Gireń, J. Steller, Investigations of the cavitation resistance of selected materials by the rotating disk method, The Szewalski Institute of Fluid Flow Machinery Polish Academy of Sciences Rep. 303/2014 (in Polish).

[51] J. Steller, Cavitation loadings at the set-ups exploited in the International Cavitation Erosion Test, The Szewalski Institute of Fluid Flow Machinery Polish Academy of Sciences Rep. 213/2014(in Polish).

[52] B.K. Sreedhar, S.K. Albert, A.B. Pandit, Cavitation Damage: Theory and Measurements – a review, Wear 372-373 (2017) 177-196.
DOI: https://doi.org/10.1016/j.wear.2016.12.009